Seismic Assessment of Evin-Valley Bridge by 3-D Inelastic Dynamic Analysis

Fakhredin Danesh[1] and Iraj Rahimi[2]

1. Assistant Professor, K.N. Toosi University of Technology, Tehran, Iran, P.O. Box 15875-4416, email: danesh@mche.or.ir
2. Former Graduate Student of Earthquake Engineering, No. 25, 12th Street, Kuye Aghajari, Ahvaz, Iran, email: irajrahimi@yahoo.com

ABSTRACT: *Major damage was observed mostly in the older bridge structures in the Northridge (1994), Kobe (1995) and Taiwan (1999) earthquakes. The most extensive damage included flexural/shear failure of substructure members and superstructure unseating at simple supports or expansion joints. In general, similar types of damages demonstrate a similar nature in view of the seismic behavior of older bridge design in all three earthquakes. As modern bridges have not been significantly affected during the recent ground motions, no reliable judgment could be made on the seismic performance of modern bridges structures.The seismic performance of Evin-Valley Bridge, a newly built slab-on-girder bridge is investigated analytically at the damage control limit state. A 3-D model of the bridge was built in DRAIN 3DX computer programme using a fiber-section beam-column element to represent inelastic behavior of RC substructure members. Elastomeric bearing pads, shear keys, expansion joints and the abutment backwalls were included in modeling of cyclic behavior of each component. The superstructure girder-beams were assumed to remain elastic and compressive elastic springs were used to represent the soil effect. A free vibration analysis of the multiple-part structure, assuming open gaps and expansion joints, showed the combined influence of a broad number of modes of vibration in dynamic response of the bridge. However, since the gaps are predicted to frequently close and reopen under earthquake forces, such results should not be relied on predicting of the seismic response. The results obtained from dynamic analyses using the Naghan (1977), the Northridge (1994) and the Kobe (1995) acceleration records show that the seismic demand values in the substructure elements are much less than the existing member capacities. The results also indicate that the dynamic response values are not comparable with the earthquake demands obtained from the equivalent static method and a large difference is observed between the results of two methods.*

Keywords: Bridge damages; Bridge modeling; Fiber elements; Inelastic analysis; DRAIN-3DX

1. Introduction

Essential shortcoming in the old seismic design approach of bridge structures has been demonstrated repeatedly by the experience of large earthquakes within the last decade around the world. After San Fernando, California, 1971 earthquake, which caused extensive damage to highway bridges a great deal of changes have been made into the bridge seismic design specifications. Such improvements were reasonably based on the observed defects in the damaged components.

During the major ground motions occurred within the last two decades, numerous bridges older than 20 to 30 years were strongly moved so that the structural deficiencies were clearly revealed. But new bridge

structures designed according to the modern seismic design codes were rarely found within the strong shaking areas; so it has not become feasible yet to empirically certify the appropriate seismic performance of modern bridge structures. Until such experience to be achieved, theoretical analyses are the only remaining tool.

In this research the authors tried to evaluate analytically the seismic performance of a newly built bridge based on *the damage control limit state* criteria. Such criteria allow a larger safety margin for the assessment of existing structures than for the design of new ones. Investigation for any probable flaws in the existing bridge was oriented with regard to the failures observed in the recent strong motion events.

The structure is idealized as a 3-dimensional mass-spring-damper model using the computer program *DRAIN*-3*DX* [12, 13]. Several elements are implemented in this program, which may be used to model various components of a bridge structure. These include a relatively powerful fiber-section beam-column element with distributed plasticity, suitable for reinforced concrete frame members. It is capable of representing various characteristics of *RC* members including cyclic strength decay, stiffness degradation, axial force-biaxial bending interaction and elastic shear behavior.

2. Seismic Damage to Bridges

A great number of bridges was suffered from the event of the Northridge, California, 1994 earthquake. Five bridges were collapsed due to the failure of columns or superstructure unseating; four ones damaged severely due to flexural hinging or shear failure of columns or typically flexural failure of the superstructure; seven bridges were experienced moderate damage consisting of cover concrete spalling, fracture of joint restrainers, abutment damage, crushing of shear keys, etc. [6, 9]. In a similar way many bridges were damaged in the Kobe earthquake, 1995. Other than transverse overturning of a 635-m length of Hanshin elevated expressway, numerous massive *RC* bridge columns were damaged seriously due to flexural hinging or severe shear cracking. Poor construction has been reported to be the main cause of damage in several bridges. In this event, unseating of superstructures most often occurred after fracturing of joint restrainers, failure of bearing devices or rigid-body movement of the bents due to the soil liquefaction or lateral spreading. In addition, several steel bridge substructures within the Kobe area were suffered from this event detecting wall/panel buckling of box-section columns which initiated at corner welds or other points of discontinuity [2, 1, 10]. Frequent collapse or severe damage to *RC* columns was observed also in Ji-Ji, Taiwan, 1999 earthquake. The most dramatic damage due to this ground motion was the chain-like falling down of the simply supported spans in a great number of bridges where no restraint was provided against longitudinal or transverse movement [7].

In all three events, the reason of collapsed or significantly damaged bridges is that all the structures were designed according to former codes. The column failure is reported to be mainly due to low lateral confinement or poor anchorage of reinforcements which imply insufficient flexural ductility, unreliable flexural strength or low shear strength. Uncertainties have been expressed on the probable influence of the vertical component of the ground motions in major damage observed in some bridge columns due to shear-axial force interaction [11]. Unseating of superstructure at simple supports is assigned to insufficient seat length or lack of restraining against horizontal movement both in transverse and longitudinal directions.

The reader may refer to Rahimi [16] for a complete review and classification of the damage caused by the recent-decade earthquakes in different bridge components. Besides to the observed local defects such as inadequate shear strength, it seems that a major shortcoming in the older bridges is the inappropriate distribution and transfer of induced forces between the different components of the structure. An example is the absorption of a large shear force to the short end columns or collapse of the superstructure after failure of a primary member of the substructure. This requires an essential revision of the design philosophy of the whole structure.

Based on the above description of the structural performance of bridges during the recent earthquakes in the following investigation, it is tried to evaluate the response of the substructure members as the major energy-dissipating component of the bridge. In addition, possible loss of support at simple supports of the existing superstructure will be of interest.

3. Description of Evin-Valley Bridge

The structure under consideration is a slab-on-girder highway bridge at north of Tehran crossing the Evin Valley in the east-west direction. The bridge was designed according to AASHTO-1991 specifications and was opened in October 1999. Figure (1) provides

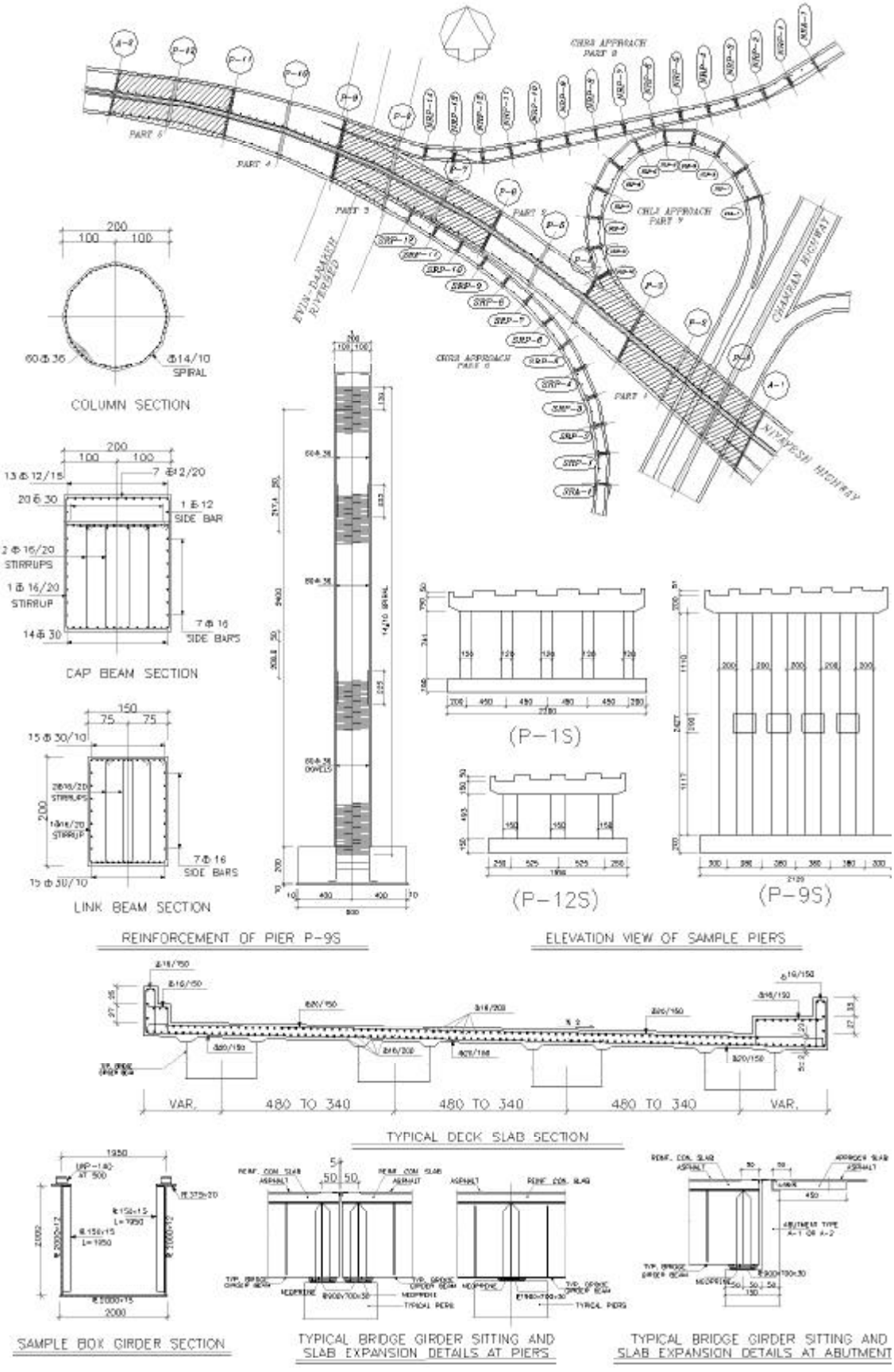

Figure 1. Plan view and typical detailing of Evin-Valley Bridge.

a plan of the intersection and typical detailing of the bridge. It consists of two adjacent structures, 2.5*m* apart. The north structure includes a main lane attached to a ramp-way and a loop-way connecting the bridge to the Chamran highway. The south one comprise of a main lane and an access ramp-way southward. Abutments of the north and south main lanes rest adjacent to each other. As in this research, only the south structure is modeled separately, a short description of the different components is presented. Each of the 13 spans of the main lane is approximately 40 m long while the ramp-way includes 13 spans of nearly 20*m* length. Substructure consists of multi-column *RC* bents with cap beams. A link beam is added at mid-height of the columns in tall bents. Table (1) summarizes dimensions of the bent members along with the reinforcement of column sections. All columns are transversely reinforced by a F14-bar spiral of 10*cm* pitch.

The superstructure constitutes of composite steel-concrete box girder beams. Steel *U* shaped sections are 2*m* wide, 2*m* deep in the main-lane spans and 1*m* deep in the ramp-way spans. Constant *RC* slab thickness is 20*cm*. 5*cm*-wide expansion joints are provided at *P*-3*S*, *P* 6*S*, P 9S and *P* 11*S*; girders continuously sit on the other bents. All ramp-way spans are simply supported. All abutments are of the simple seat type. Elastomeric bearing pads are provided at all supports in the main lane but girder beams rest on steel sitting plates in the ramp-way. In addition, shear keys are present between each two adjacent girders to restrict lateral slip at all supports with an initial gap of 10*cm* width.

Foundations consist of shallow rectangular strip footings, typically 1.5 or 2*m* thick. Length and width of the footings is variable and both top and bottom reinforcement mats are provided.

Material properties are as follows: $f_c' = 20\ MPa$; $f_y = 400\ MPa$ and $f_u = 600\ MPa$ for reinforcement bars; $f_y = 240\ MPa$ for steel plates; $E_{steel} = 206000\ MPa$.

4. Structural Modeling

Among the elements included in *DRAIN*-3*DX*, elements *TYPE* 01 (inelastic truss element), *TYPE* 05 (friction bearing element), *TYPE* 09 (link element with gap and tension/compression option), *TYPE* 15 (inelastic fiber beam-column element) and *TYPE* 17 (elastic beam-column element) were used to model different components of the Evin-Valley Bridge.

Substructure bents including columns, cap beams and link beams were idealized at centerlines by element *TYPE* 15. The base node of the columns locates at the foundation centerline. A rigid end zone connects each column base to the foundation top level. Reinforced concrete section of columns is discretized into steel and concrete fibers in a radial pattern as shown in Figure (2). Moment-curvature

Table 1. Dimensions and reinforcements of bent members in the south main bridge.

Bent	h_{clear}(m)	d_{col}(m)	Column	Cap Beam	Link Beam
P-1S	7.41	1.2	20Φ32	150 x 150	-
P-2S	9.96	1.5	24Φ32	200 x 150	-
P-3S	13.65	1.5	28Φ32	200 x 150	120 x 150
P-4S	15.74	2.0	34Φ36	200 x 200	150 x 200
P-5S	16.65	2.0	34Φ36	200 x200	150 x 200
P-6S	17.54	2.0	40Φ36	200 x 200	150 x 200
P-7S	18.47	2.0	40Φ36	200 x 200	150 x 200
P-8S	24.00	2.0	60Φ36	200 x 200	150 x 200
P-9S	24.27	2.0	60Φ36	200 x 200	150 x 200
P-10S	14.74	1.5	42Φ36	200 x 150	120 x 150
P-11S	8.14	1.5	24Φ32	200 x 150	-
P-12S	4.93	1.5	18Φ32	200 x 150	-
SRP-1 to SRP-5	6.19 ~ 12.11	1.5	28Φ32	200 x 150	-
SRP-6 to SRP-12	14.56 ~ 20.49	2.0	48Φ32	200 x 150	150 x 200

evaluation of a sample section can be accurate with increasing number of fibers and it is shown that 41 concrete fibers and 16 steel fibers can be practically adequate. Figure (3a) illustrates the influence of section refinement on the response *M-f* curves. Similarly, the output results are sufficiently accurate if each fiber-section element is divided into 10 segments along its length, see Figure (3b). The same procedure was used for cap/link beams but each element should be divided into 5 segments with slight permission of error for analysis time saving.

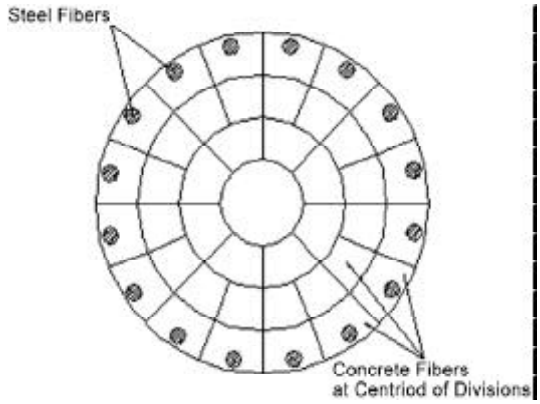

Figure 2. Circular-section discretization into concrete and steel fibers.

Theoretical model recommended by Mander et al [8] for the stress-strain relationship of confined concrete was used to define the inelastic behavior of concrete fibers. Figure (4a) represents f_c-e_c curve for three column section types. A method suggested by Mander et al [8], is used to calculate the ultimate strain of concrete at the damage control limit state which is governed by the fracture of transverse reinforcements. A numerically-solved equation of energy equilibrium is considered in this method.

Because of convergence problems, modeling of cover concrete as unconfined material, as well as concrete tensile strength was ignored. Mander et al [8] also provide factors to modify f_c-e_c curve for dynamic loading. For this case, dynamic loading factors for strength, stiffness and strain are 1.19, 1.11 and 0.89 respectively. As shown in Figure (4b), stress-strain behavior for steel fibers is symmetric in tension and compression.

The superstructure of the bridge was modeled as a grid of elastic beams by element *TYPE* 17. Idealized linear elements pass through the centroid of

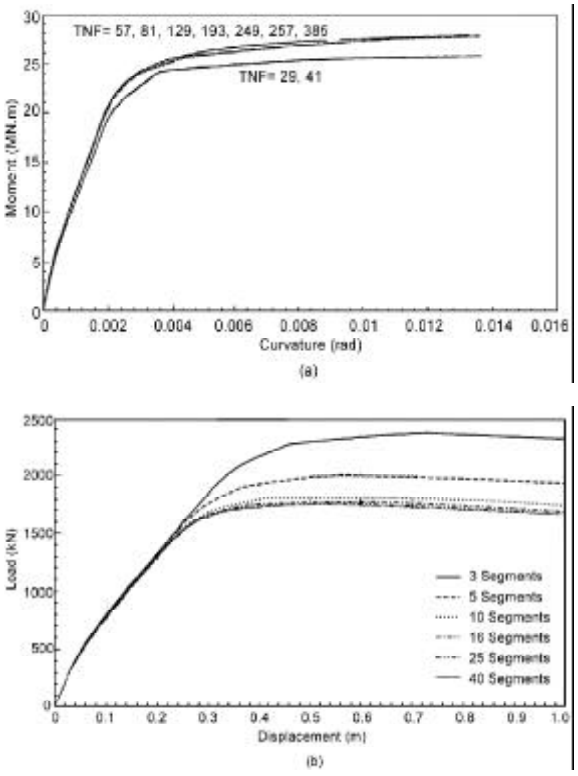

Figure 3. a) Influence of increasing number of fibers on the section moment-curvature response (TNF means total number of fibers); b) Influence of increasing number of segments on the element load-displacement response.

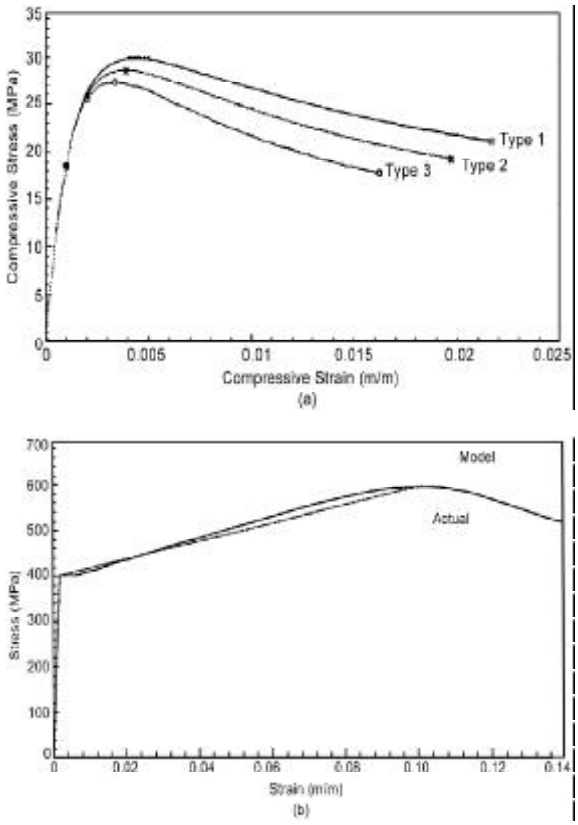

Figure 4. a) Stress-strain curves for concrete fibers in column sections based on Mander et al [8] model; b) Stress-strain behavior of steel fibers.

longitudinal girder beam sections. Transverse beams representing bending stiffness of the concrete slab between adjacent girder beams spaced at 0.2 l (l = span length) in the main lane spans and 0.25 l in the ramp-way spans. At expansion joints, element *TYPE* 09 were used to represent the effect of pounding when the initial gap is closed. Stiffness of such elements after gap closing was assumed identical to the elastic axial stiffness of the *RC* slab.

The elastomeric bearing pads and the shear keys were idealized, as outlined in Figure (5), using element *TYPE* 05 and *TYPE* 09 respectively. Element *TYPE* 05 has two components: a bearing component and a friction component. For simplicity, all shear keys at a support were collectively represented by two elements. Shear capacity of each element is the total value of all keys at a support $V_{key} = I_s \mu f_y \sum A_s$ where shear stress reduction factor $f_s = 1$ and Coulomb friction coefficient $P = 1.4$ are assumed. $\sum A_s$ is the total area of the bars dowelled into the underlying cap beam.

The element *TYPE* 09 was used for modeling of the effect of the passive soil pressure behind the abutments on the seismic response of the bridge when the initial gap between the superstructure and the abutment backwall is closed. For the abutments *A*-1*S*, *A*-2*S,* and *SRA*-1, the nonlinear change of soil pressure after gap closing was based on the Maroney-Chai dimensionless curve [14] as illustrated in Figure (6).

Equivalent elastic springs idealize soil response effects on the structure. The proposed model of Chen [5] was used to calculate spring constants. Neglecting the effect of the rotational modes of foundation vibration, translational springs were defined parallel to the local coordinates of each bent. Element *TYPE* 09 was used to model the soil springs responding only in compression; a gap will open under tension. A perspective view of the finalized model is shown in Figure (7).

Structural mass within superstructure, bent members and foundations was lumped at the corresponding nodes. Table (2) summarizes the structural mass data. Free vibration analysis of the model assuming open gaps resulted in a broad number of effective modes of vibration with the first predominant modes in the global X and Y directions contributing only 36% and 12% respectively. Another analysis with closed gaps resulted in much different values for periods and the effective modal mass ratios as compared in Table (3) for the first 20 modes of vibration where the governing modes in two

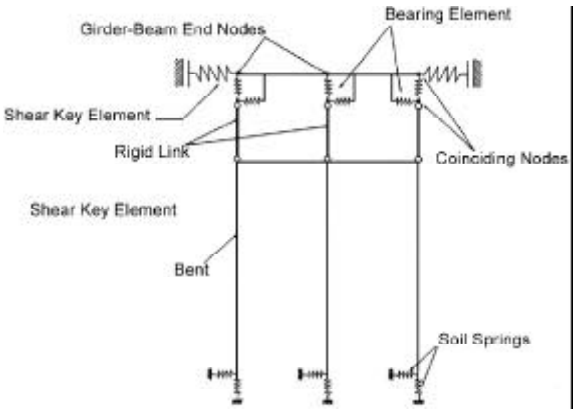

Figure 5. Modeling of the bearing systems and soil effects.

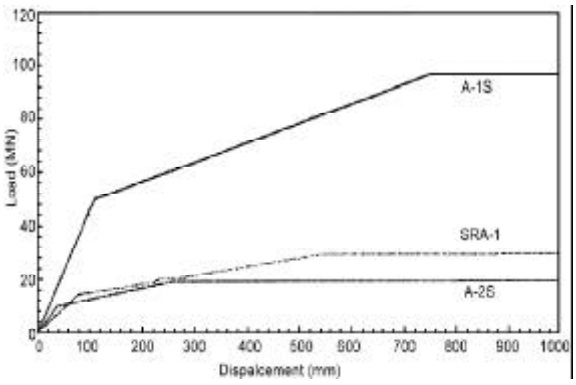

Figure 6. Load-displacement behavior of abutment backwall springs.

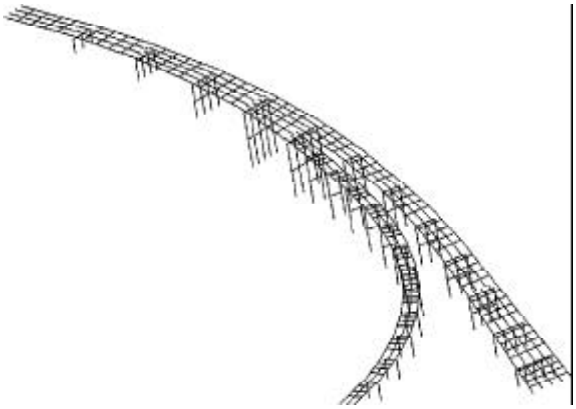

Figure 7. A perspective view of the assembled model.

orthogonal directions contribute 68% and 60% respectively. At the beginning of seismic response, all gaps are open but gap closing seems to occur frequently under seismic loading. While a structure-state with all closed gaps does not seem to be a matter of reality, free vibration analysis of the open-gap structure just sorts the independent modes of vibration

of the multiple parts of the structure separated by expansion joints. Whilst the earthquake waves arrive at the site, individual parts will start to vibrate almost at the same time. Therefore, no one of the two output sets describes the vibration response of the bridge in a rational manner and no one should simply be used to predict the probable dynamic response. These analyses also confirmed the slight effect of the foundations mass but more pronounced contribution from the bents especially in higher modes of vibration.

5. Inelastic Dynamic Analysis

Gravity loads including superstructure and sub-structure weight were applied as concentrated force at corresponding nodes since no option is provided in *DRAIN-3DX* to distribute loads along linear elements. Dynamic analysis was carried out using three horizontal earthquake acceleration records: (1) Naghan, Iran, 6 April 1977, Figure (8a) (2) Northridge, California, 17 January 1994, Rinaldi

Table 2. Contribution of different parts of the structure to the total mass.

Bridge Part	Main Lane		South Ramp	
	Mass (Tons)	Percent of Total	Mass (Tons)	Percent of Total
Superstructure	8861	29.16	2949	9.71
Bents	6514	21.44	3519	11.58
Foundations	5219	17.18	3321	10.93
Total	20549	67.63	9789	32.37

Table 3. Period and effective modal mass ratio for the first 20 modes of vibration.

Mode	Open Gaps			Closed Gaps		
	Period (s)	X	Y	Period (s)	X	Y
1	1.531	0.3696	0.0318	1.080	0.6859	0.0038
2	1.407	0.1674	0.0508	0.996	0.1383	0.0404
3	1.316	0.0009	0.0000	0.970	0.0229	0.6043
4	1.268	0.0698	0.0146	0.915	0.0273	0.0088
5	1.087	0.0866	0.0048	0.784	0.0028	0.1476
6	1.061	0.0028	0.1206	0.676	0.0230	0.0053
7	1.054	0.0028	0.0181	0.496	0.0018	0.0207
8	1.037	0.0350	0.1469	0.385	0.0025	0.0042
9	1.013	0.0168	0.0502	0.387	0.0000	0.0000
10	1.004	0.0072	0.0044	0.364	0.0000	0.0000
11	1.001	0.0070	0.0969	0.357	0.0050	0.0794
12	0.991	0.0021	0.0156	0.346	0.0138	0.0047
13	0.961	0.0001	0.0004	0.339	0.0000	0.0000
14	0.922	0.0237	0.0612	0.325	0.0285	0.0706
15	0.772	0.0005	0.2027	0.318	0.0000	0.0000
16	0.691	0.0726	0.0087	0.296	0.0013	0.0006
17	0.470	0.0001	0.0540	0.296	0.0028	0.0010
18	0.388	0.0000	0.0000	0.285	0.0000	0.0000
19	0.387	0.0011	0.0004	0.277	0.0000	0.0000
20	0.385	0.0000	0.0000	0.271	0.0073	0.0009
Total	-	0.8660	0.8822	-	0.9632	0.9915

receiving station, Figure (8b); and (3) Kobe, Japan, 17 January 1995, *JMA* station, Figure (8c). All records were scaled to the design basis acceleration of 0.35*g* at Evin-Valley Bridge site by BHRC [4]. Strong motion duration was restricted by the "bracketed duration method" to be 4.40, 14.85 and 17.68 seconds respectively for the Naghan, Northridge and Kobe records. Figure (9) compares

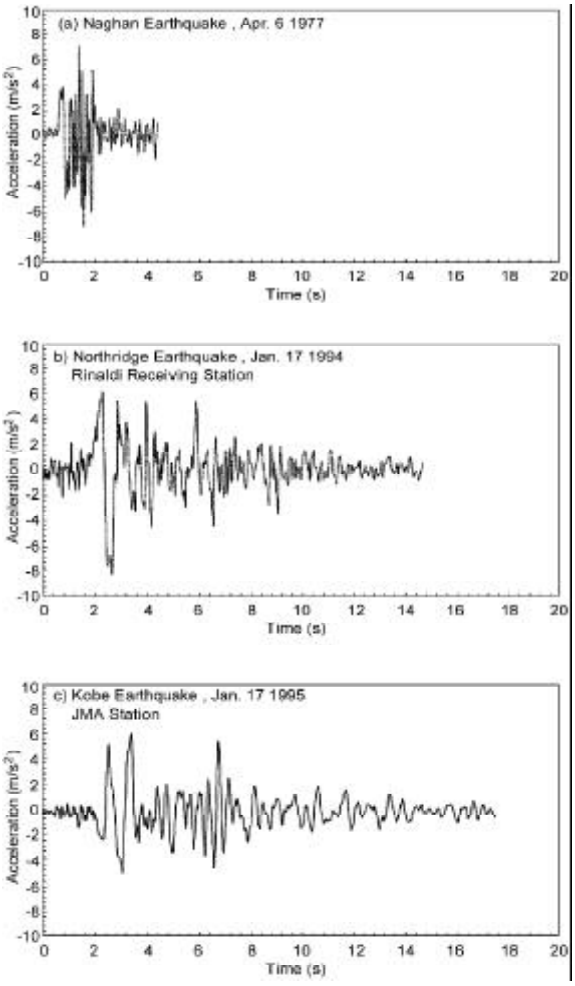

Figure 8. The acceleration time-histories of the applied ground motions.

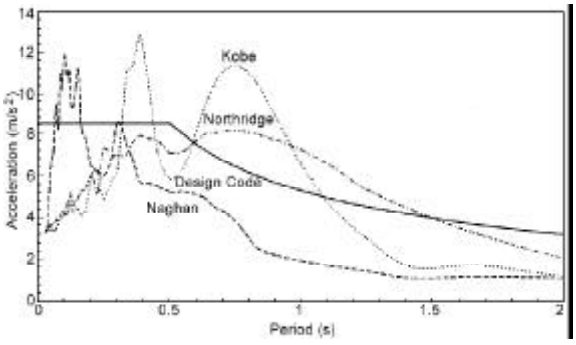

Figure 9. A comparison of the response spectra to the design spectrum.

the elastic response spectra for the three records to the design spectrum. It is evident that the Naghan record will excite very short periods of vibration more than two other acceleration records while the Northridge and Kobe records cause longer-period modes to be excited even more severe than the design spectrum. At first the Naghan record was applied to the structure in four horizontal directions: (1) 1.0*L*, (2) 1.0*T*, (3) 1.0*L*+0.3*T* and (4) 0.3 *L* + 1.0 *T*, hereafter denoted as *LC*1, *LC*2, *LC*3 and *LC*4. *L* and *T* stand for longitudinal and transverse directions respectively. Since it was observed that the response of the bridge due to seismic loading in *LC*1 and *LC*3 directions differ slightly and the same is true for *LC*2 and *LC*4 directions, the analyses under the Northridge and Kobe records were carried out only for *LC*3 and *LC*4 directions. Iranian code for seismic loading of highway bridges [3] ignores vertical component effects and requires only consideration of *LC*1 and *LC*2.

With automatic time-stepping scheme and a force error tolerance of 0.1*kN*, each analysis took about 190 hours long for the Naghan record and 480-530 hours long for the first 9 seconds of the Northridge and Kobe records on a 750 *MHz* Pentium *III PC*.

6. Analytical Results and Discussion

Typical time-history results are given in Figures (10) through (13). Figure (10) illustrates the time-history of the bending moment in the critical section of a column of bent *P*-8*S* both for *LC*3 and *LC*4 directions. In Figure (11) the horizontal displacement time-history is shown for the top node of bent *P*-8*S* under the Northridge ground motion in directions perpendicular and parallel to the plane of the bent respectively in part (a) and (b). To investigate the risk of the superstructure unseating at simple supports during the motion, slippage of the girder-beam ends on the elastomeric bearings is of interest. Figure (12) illustrates the time variation of the displacement of girder-beam end nodes relative to the underneath support at the abutment *A*-1*S*. Again the results are given in two orthogonal directions along the support line and perpendicular to line of support. Similar results may be observed in Figure (13) at the expansion joint on the bent *P*-8*S* .

A review of the inelastic events occurred during the seismic loading showed that under the Naghan record no reinforcement yielding took place in neither

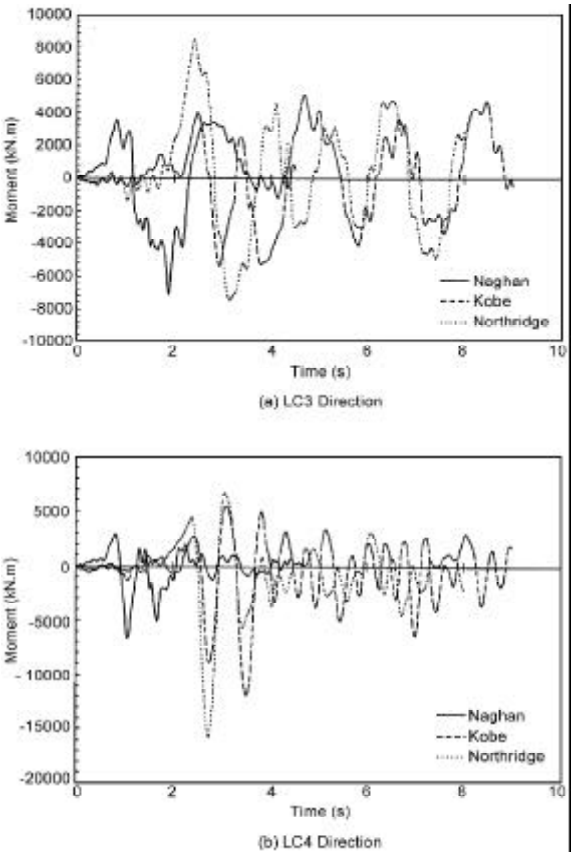

Figure 10. Time variation of the bending moment in a column of bent P-8S.

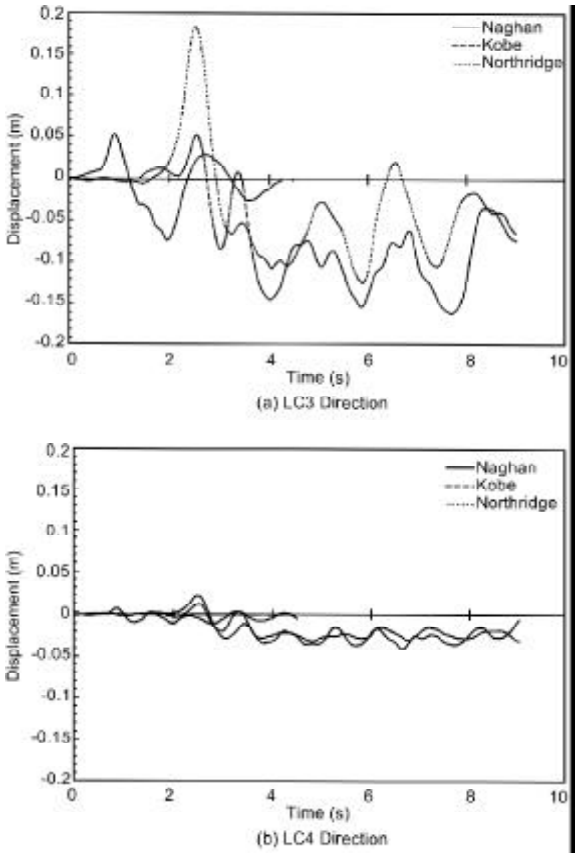

Figure 12. Time variation of the girder-beam end slippage at the abutment A-1S.

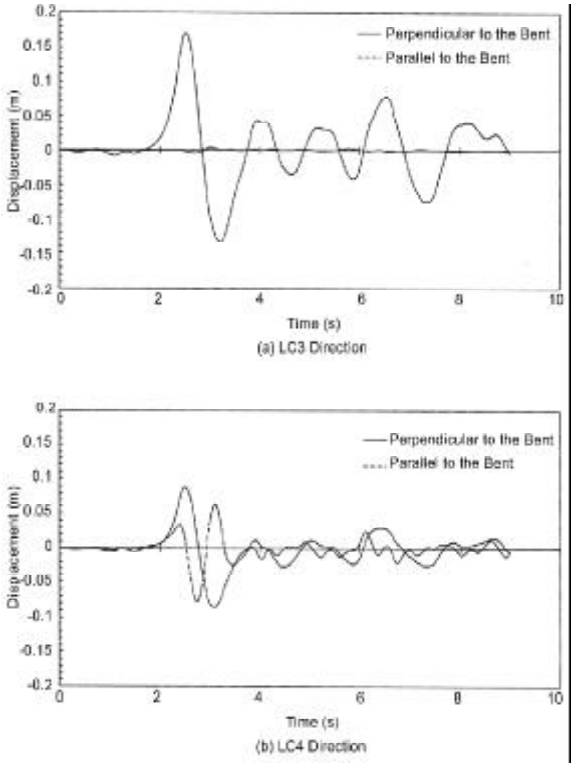

Figure 11. Time variation of the displacement at the top of the bent P-8S under the Northridge ground motion.

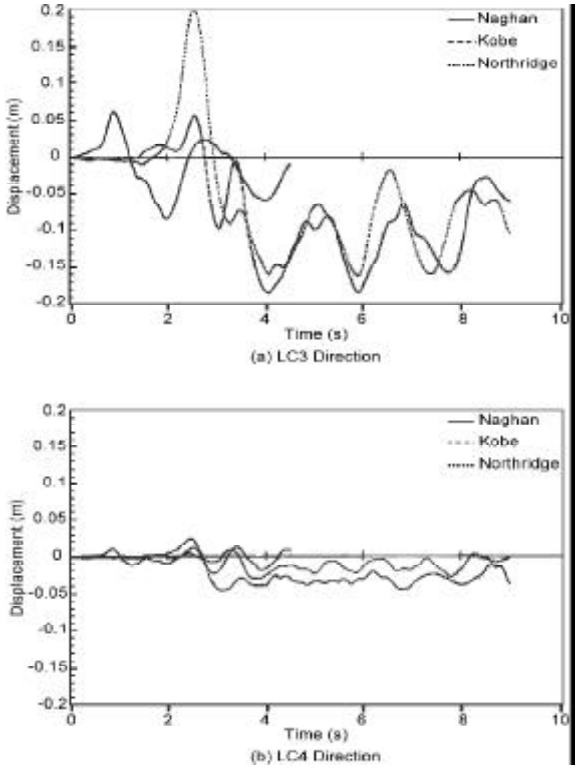

Figure 13. Time variation of the girder-beam end slippage at the joint on the bent P-8S.

columns nor cap/link beams but compressive/tensile yielding of bars and concrete cracking occurred under the Northridge and Kobe records. In addition, compressive yielding of concrete has come about only under the Northridge record in $LC3$ direction. The beam girders slipped frequently on the bearing pads for loading in both longitudinal and transverse directions. In the shear-key elements the initial gaps closed/opened repeatedly when the structure was excited in transverse direction. The response of expansion-joint elements included frequent cumulative opening.

Figures (14) and (15) compare the maximum bending moment induced in a series of sample column members by different earthquakes to M_{EQ}, M_{design}, M_{ucode} and M_u respectively for $LC3$ and $LC4$ directions. M_{EQ} is the bending moment demand determined by the equivalent static method of analysis and used for structural design. M_{design} denotes the bending moment value used for design of the column sections; it combines M_{EQ} with the effects due to other loading types and possibly slenderness of the column. M_{ucode} is the bending moment capacity of the section specified by ACI-318 for an ultimate concrete strain of 0.003. M_u refers to a more precise value for the moment capacity calculated based on the section discretization into fibers and using the precise stress-strain curves for concrete and steel fibers (taking account of the dynamic effects and the strain-hardening effects). Axial force due to gravity loads was used to calculate both M_{ucode} and M_u.

It is observed that M_{ucode} and M_u differ slightly but M_u is much greater than M_{design}. In Figure (16), the ratio of M_u/M_{design} is given for the column section of the different bents of the bridge. It clearly demonstrates that the substructure of the bridge holds a large margin of safety when the strength capacity is compared to the strength demand values determined by the equivalent static method of analysis. This observation may justify the foregoing observation of slight inelastic response of the bents under the applied earthquake records which were scaled to the design basis acceleration.

Remarkably a considerable difference is observed if one compares M_{EQ} values to the dynamic response of the members both in $LC3$ and $LC4$ directions. This comparison seems reasonable since the dynamic response values do not include the code-specified magnification due to slenderness effects. In addition, the bending moment induced by the gravity in the columns of a short-span multi-column bent, such as in Evin-Valley Bridge, is rather small when compared to the lateral loads. Even the Naghan ground motion which did not cause significant inelastic flexural response has resulted in the bending moment to exceed M_{EQ} in some sample members. For the Northridge and Kobe records, the response values exceed M_{EQ} up to more than 200% in a number of sample column members. This is evident in both Figures (14) and (15).

In Figure (17) the maximum curvature ductility

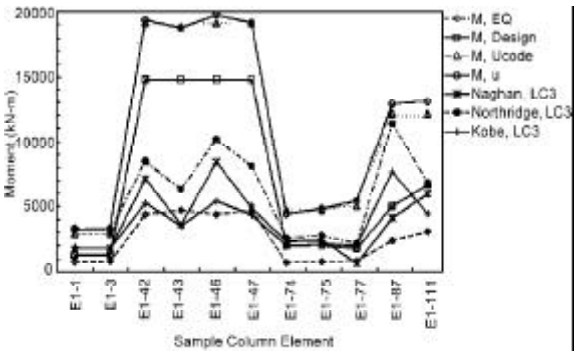

Figure 14. Maximum bending moments in selected column members and comparison to the section capacities and design forces.

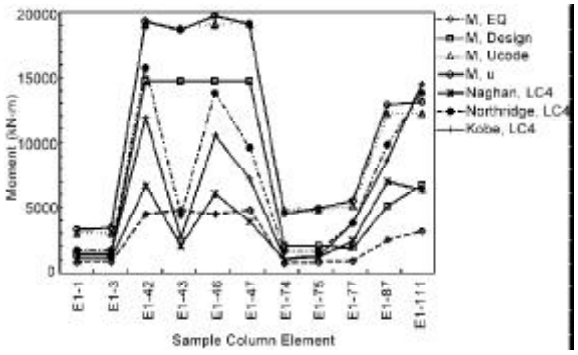

Figure 15. Maximum bending moments in selected column members and comparison to the section capacities and design forces.

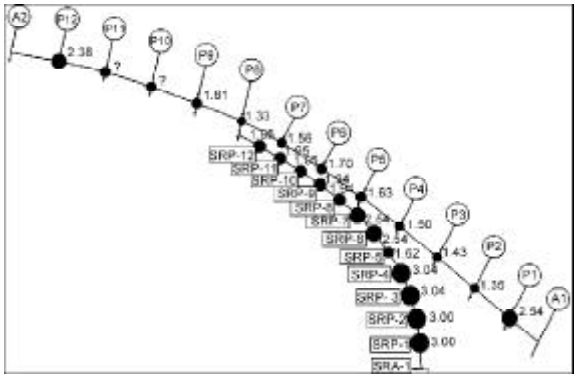

Figure 16. The ratio of M_u/M_{design} for different bents of Evin-Valley Bridge.

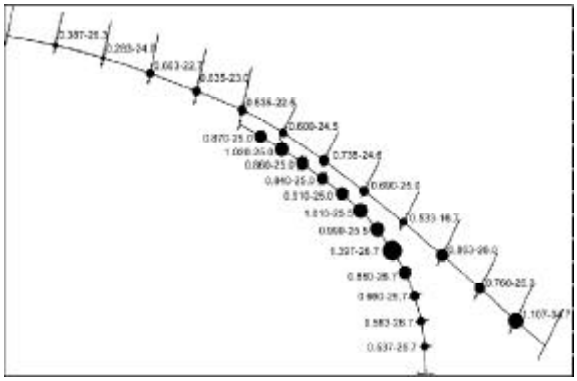

Figure 17. m_{demand} (first number) and $m_{capacity}$ (second number) for different bents of Evin-Valley Bridge.

demand, μ_{demand}, experienced in the columns of the different bents due to ground acceleration records applied to the structure is given along with the curvature ductility capacity, $\mu_{capacity}$, of the column sections. The curvature ductility capacity is at the damage control limit state governed by the fracture of transverse reinforcements as defined previously. Only in a few number of bents, μ_{demand} exceeds 1.0. A large difference there exists between μ_{demand} and $\mu_{capacity}$. The ductility demand values does not change in a predictable manner along the bridge. While the bent *P*-12*S* experiences a low ductility demand, it exceeds 1.0 at the other end short bent *P*-1*S*. However, the values of ductility capacity seem to follow a more smooth variation.

BHRC [3] recommends equivalent static method of analysis under earthquake forces for a series of regular bridges. Abrupt change in mass distribution, variation of stiffness between two adjacent bents by more than 25% relative to the more flexible bent and a horizontal arch angle of greater than 90º causes a bridge to be categorized as irregular. Pseudo-dynamic (spectral) or dynamic method of analysis should be used for regular curved, suspension or cable-stayed bridges and irregular bridges of spans less than 150*m*.

As indicated in Table (4), because of the sudden

Table 4. Change in stiffness of each bent of the Evin-Valley Bridge relative to the next bent.

Bent	Stiffness Change Relative to the Next Bent
P-1S	0.085
P-2S	0.15
P-3S	0.241
P-4S	0.132
P-5S	0.140
P-6S	0.106
P-7S	0.052
P-8S	0.018
P-9S	0.188
P-10S	0.458
P-11S	1.390
P-12S	-

change in the relative lateral stiffness of the adjacent bents, the Evin-Valley Bridge goes into the category of short-span irregular bridges and it should not be analyzed simply by the equivalent static method. Prior to an initial design of the substructure, relative lateral stiffness of the bents is not known and the equivalent static method will possibly be used for estimation of the seismic demands. However, it seems necessary to check the final design to comply with the code provisions. While the authors pointed to the problems encountered in the free vibration analysis of the multiple-part structures, BHRC [3] does not provide any specification or recommendation for the professional engineer for reliable estimation of the dynamic response of the bridge using pseudo-dynamic or dynamic methods of analysis.

An evaluation of the critical shear force in the substructure members also revealed a large difference to the existing capacities as estimated using the procedure recommended by Priestley et al [15]. Interested readers may refer to Rahimi [16] for details.

In Table (5) the maximum girder-beam end slippage perpendicular to the line of the support is

Table 5. Maximum girder-beam end slippage at selected simple supports perpendicular to the line of the support (in cm).

Support	Naghan				Northridge		Kobe		Seat Length
	LC1	LC2	LC3	LC4	LC3	LC4	LC3	LC4	
A-1S	7.0	0.9	7.3	2.3	18.3	6.8	16.2	3.6	85
A-2S	5.9	1.3	6.9	2.7	14.7	8.5	10.7	6.2	85
P-6S	8.3	0.3	8.4	2.8	20.1	5.9	18.4	5.2	80
SRA-1	0.8	1.5	0.4	1.2	1.3	4.5	1.3	3.8	80
SRP-6	5.2	2.8	5.0	1.0	19.1	4.1	9.2	4.3	85

given along with the seat length at selected simple supports. Comparing the values of slippage to the available seat lengths shows that the superstructure is not at the risk of unseating when the bridge is excited with the applied ground motions.

7. Conclusions

Based on the analyses carried out on a complex 3-*D* model of the Evin-Valley Bridge described in this paper a series of conclusions may be drawn:

- The assumption of open or closed expansion joints affects considerably on the results of free vibration analysis of Evin-Valley Bridge. Such results for a multiple-part bridge where expansion joints between the parts will possibly close/open frequently under earthquake loading may not describe the actual vibration response of the bridge and they should not be used for evaluation of the seismic demands before proper validation.
- Expansion joints and shear-key gaps in Evin-Valley Bridge closed and opened repeatedly under the applied earthquake acceleration records. Further research is needed to evaluate the amount of contribution from each component to the total response.
- The capacity of the substructure in Evin-Valley Bridge is by a large amount greater than that required by the seismic demands estimated using the equivalent static method of analysis, which may exhibit a large margin of safety against the design earthquake. At the same time, internal forces in the substructure members obtained from dynamic analyses are much larger than forces predicted by the equivalent static method; the difference is more than 100% or 200% in some columns. Such substantial differences may neutralize the above safety margin.
- Although by the code requirements, the bridge should have been analyzed by the pseudo-dynamic method but there is no recommendation for modeling of such multiple-part bridges in order to obtain reliable results whereas free vibration analysis is a prerequisite to the pseudo-dynamic analysis. Linear structural analysis programs are not suitable for modeling of gaps in the structure while nonlinear analyses are more complicated and time-consuming to be used in a design office. It seems that much more research is required to develop simplified analysis procedures, which take into account such effects due to gaps/joints in estimation of seismic demands on a multiple-part bridge structure.

Acknowledgements

The authors would like to thank Mr. Amir-Payman Zandi (P.E.) and Dr. Behrouz Asgarian, both lecturers at the Department of Civil Engineering, K. N. Toosi University of Technology, Prof. Gregory L. Fenves, University of California at Berkeley and Prof. Giorgio Monti, University of La Sapienza at Rome, for providing useful suggestions during the research reported in this paper.

References

1. Abe, S., Fujino, Y., and Abe, M. (2000). "An Analysis of Damage to Hanshin Elevated Expressway During 1995 Kobe Earthquake", *Proceedings 12th World Conference on Earthquake Engineering*, Auckland, New Zealand, Computer File.

2. Anderson, D.L., Mitchell, D., and Tinawi, R.G. (1996). "Performance of Concrete Bridges During the 1995 Hyogo-Ken Nanbu (Kobe, Japan) Earthquake", *Canadian Journal of Civil Engineering*, **23**(3).

3. Building and Housing Research Center (1996). "Code of Practice for the Earthquake Resistant Design of Road and Railroad Bridges", Tehran: BHRC (in Persian).

4. Building and Housing Research Center (1998). "Iranian Code of Practice for Seismic Resistant Design of Buildings", 2nd Edition, Tehran: BHRC (in Persian).

5. Chen, Y. (1996). "Modeling and Analysis Methods of Bridges and Their Effects on Seismic Responses: I—Theory", *Computers and Structures*, **59**(1).

6. Earthquake Engineering Research Institute (1995). "Northridge Earthquake of January 17, 1994 Reconnaissance Report", *Earthquake Spectra*, Supplement C, **11**.

7. Mahin, S. (1999). Preliminary Reconnaissance Report of Taiwan, Ji-Ji Earthquake of September 1999, Via Internet: http://www.eerc.berkeley.edu.

8. Mander, J.B., Priestley, M.J.N., and Park, R. (1988). "Theoretical Stress-Strain Model for Confined Concrete", *J. of Structural Engineering, ASCE*, **114**(8).

9. Mitchell, D., Bruneau, M., Williams, M., Anderson, D. Saatcioglu, M., and Sexsmith, R. (1995). "Performance of Bridges in the 1994 Northridge Earthquake", *Canadian Journal of Civil Engineering*, **22**(2).

10. Motoki, K. and See, K. (2000). "Strong Motion Characteristics Near the Source Region of the Hyogoken-Nanbu Earthquake from Analysis of the Directions of Structural Failure", *Proceedings 12th World Conference on Earthquake Engineering*, Auckland, New Zealand. Computer File.

11. Papazoglu, A.J. and Elnashai, A.S. (1996). "Analytical and Field Evidence of the Damaging Effect of Vertical Earthquake Ground Motion", *Earthquake Engineering and Structural Dynamics*, **25**(10).

12. Powell, G.H. and Campbell, S. (1994). "Drain-3DX Element Description and User Guide for Element Type 01, Type 04, Type 05, Type 08, Type 09, Type 15 and Type 17", University of California at Berkeley, Report No. UCB/SEMM-94/08.

13. Prakash, V., Powell, G.H., and Campbell, S. (1994). "Drain-3DX Base Program Description and User Guide", University of California at Berkeley, Report No. UCB/SEMM-94/07.

14. Priestley, M.J.N., Seible, F., and Calvi, G.M. (1996a). "Seismic Design and Retrofit of Bridges", New York, John Wiley and Sons.

15. Priestley, M.J.N., Verma, R., and Xiao, Y. (1996b). "Seismic Shear Strength of Reinforced Concrete Bridge Columns: Closure by the Authors", *J. of Structural Engineering*, *ASCE*, **122**(4).

16. Rahimi, I. (2001). "Seismic Assessment of Evin-Valley Bridge by Inelastic Dynamic Analysis", M.Sc. Dissertation, K.N. Toosi University of Technology, Tehran, Iran (in Persian).